Synthesis and characterization of nickel cobalt ferrite nanoparticles via heat treatment method

Vishal K. Chakradhary[1*], Azizurrahaman Ansari[1], M. J. Akhtar[1, 2]

[1]*Materials Science Programme, Indian Institute of Technology, Kanpur, Uttar Pradesh, 208016, India*
[2]*Department of Electrical Engineering, Indian Institute of Technology, Kanpur, Uttar Pradesh, 208016, India*

[*]Corresponding author, E-mail: vishk@iitk.ac.in; Tel: (+91)9580399557

Received: 30 March 2016, Revised: 01 August 2016 and Accepted: 03 August 2016

DOI: 10.5185/amp.2016/114
www.vbripress.com/amp

Abstract

Material synthesis is a scientific art, considering all parameters and conditions in practical view and applying them in an experiment. Properties of synthesized material can be tuned further by technically playing with concerned parameters individually. In this work, a one to one relation between the formation of cubic spinel ferrite structure with stable phase and morphology has been established, and corresponding changes in the magnetic properties are investigated with temperature. Heat treatment method is adopted for the preparation of nanoparticles of cobalt doped nickel ferrite $Ni_{1-x}Co_xFe_2O_4$ (x=0.5) and characterized by XRD, FESEM, TGA and VSM. Initially, as synthesized powder sample shows amorphous and weak ferromagnetic nature (M_s = 0.04 emu/g, H_c = 92.42 Oe), but heat treatment at 400ºC exhibits signature of phase formation with irregular particle shape and ferromagnetic (M_s = 6.62emu/g, H_c = 460 Oe) behaviour. On further heating upto 600ºC, the nanoparticles of $Ni_{1-x}Co_xFe_2O_4$ (x=0.5) is formed with stable cubic spinel crystal structure (lattice constant a=8.35452Å) and enhanced magnetic properties (M_s=8.24emu/g, H_c=1955Oe). Due to higher coercivity obtained of $Ni_{1-x}Co_xFe_2O_4$ (x=0.5) nanoparticles, it may be useful material in the production of data storage devices, permanent magnet, parts of electronic circuits and also in stealth technology.

Keywords: Heat treatment, nickel cobalt ferrite, nanoparticle, inverse spinel, coercivity.

Introduction

The ferrite nanoparticles have different and unique electrical and magnetic properties than their bulk counterpart. Due to this fact, they are commercially and technologically important. The ferrite nanoparticles cover wide and diverse application areas depending upon its suitable characteristics. Because of its high coercivity and saturation magnetization, they are currently used in making the recording devices, permanent magnets, electric motors, automotive traction **[1-4]**. The various electronic parts in communication technology are fabricated using ferrite nanoparticles such as inductors, transformer core and the microwave components for electromagnetic shielding to protect sensitive devices from external electromagnetic waves **[5-8]**. Ferrite nanoparticles are also applied in chemical reactions due to their catalytic, photo catalytic, and photo electrochemical properties **[9-11]**. Recently, it is investigated that ferrite nanoparticle can be applied in biomedical field owing to its antibacterial properties **[12]**. The ferrite nanoparticles are magnetic in nature so they can move under the influence of externally applied magnetic field and they can also dissipate heat when radio frequency is applied, these properties have enabled to implement drug delivery, tissue destruction, and remote biological applications and also ferrite nanoparticles can be used in making smart nanodevices for cancer apoptosis **[13-16]**.

Spinel ferrites have general formula AB_2O_4, where A is divalent and B is trivalent metal cations respectively. The Oxygen forms a FCC crystal lattice with 32 O^{2-}, which has 64 tetrahedral and 32 octahedral vacancies, wherein, 1/8 of tetrahedral and 1/2 of octahedral sites are occupied by A and B metal cations **[17-19]**. Depending upon type and occupancy of divalent and trivalent metal cations in tetrahedral and octahedral interstices, properties of ferrites nanoparticles get changed. A number of synthesis route are now being applied to synthesize the ferrite nanoparticles such that the co-precipitation, sol-gel, auto combustion, aerosol, ceramic and thermal treatment **[20-26]**.

In this paper, cobalt doped nickel ferrite of $Ni_{1-x}Co_xFe_2O_4$ (x=0.5) is synthesized by heat treatment method. The crystal structure formation and phase stability of sintered ferrite nanoparticles at 400 ºC and 600 ºC are studied. The simultaneous change in magnetic properties such as coercivity (H_c) and saturation magnetisation (M_S) are also investigated. The objective of this work is to synthesize the cobalt doped nickel ferrite nanoparticles via heat treatment method and study their structural, morphological, thermal and magnetic properties. The synthesis method can be used in large scale to synthesize ferrite nanoparticles due to low cost processing, easy to use and time saving.

Experimental

Materials

Synthesis of cobalt doped nickel ferrite nanoparticles, includes the raw materials as hydrated cobalt nitrate ($Co(NO_3)_2.6H_2O$, purity ~ 98%) from Loba Chemie, Mumbai, hydrated nickel nitrate ($Ni(NO_3)_2.6H_2O$, purity ~ 99%) from Loba Chemie, Mumbai, and hydrated iron nitrate ($Fe(NO_3)_2.9H_2O$, purity ~ 98%) from Merck, Mumbai. The poly vinyl pyrolidone (PVP K30, M. W. ~ 40000) polymer powder Loba Chemie, Mumbai, and all chemicals are used without further purification. The deionised (DI) water is used as solvent.

Preparation of Cobalt doped nickel ferrite $Ni_{1-x}Co_xFe_2O_4$ (x=0.5) nanoparticles

In order to prepare $Ni_{0.5}Co_{0.5}Fe_2O_4$ nanoparticles, 0.05 moles of $Ni(NO_3)_2.6H_2O$, 0.05 moles of $Co(NO_3)_2.6H_2O$, and 2 moles of $Fe(NO_3)_2.9H_2O$ (1:1:2) are dissolved in 75 ml of de-ionized water each separately. Further, 9 g of poly vinyl pyrrolidone (PVP) is added in 200 ml of de-ionized water at 70 ºC and stirred till the whole PVP is dissolved. The metal nitrate solutions are then mixed into the polymeric solution (PVP solution) and stirred continuously for 2 hours at 70ºC in order to avoid the agglomeration. The PVP assists to prevent the agglomeration and hence acts as capping agent. Finally, the orange colored solution is obtained, which is then dried in an electric oven for 24 hrs. The obtained orange colored solid is crushed into powder using mortar and pestle. The synthesized powder is heat treated at 400ºC and 600ºC in order to get the ferrite nanoparticles.

$$x\,Co(NO_3)_2 + (1-x)Ni(NO_3)_2 + 2Fe(NO_3)_3 \xrightarrow[PVP]{600^oC} Ni_{1-x}Co_xFe_2O_4 + \text{other products including oxides of Nitrogen and Carbon}$$

Characterizations

X-ray diffraction (XRD) patterns of $Ni_{0.5}Co_{0.5}Fe_2O_4$ nanoparticles are recorded by x-ray diffractometer (Rigaku MiniFlex 600 model) in 2θ range of 20º-80º with Cu Kα radiation (wavelength =1.540562Å). The morphology of the synthesized ferrite nanoparticles is studied from the field emission scanning electron microscopy (FE-SEM) images. The FE-SEM (model: JSM-7100F; JEOL, SE resolution: 3nm at 15kV/5nA, and Magnification: 10x to 1000kx) is used for the microscopic imaging. The Thermo-gravimetric analysis is carried out using Perkin Elmer TG/DTA instrument with heating rate 5°C/min up to 700°C in air ambient. A vibrating sample magnetometer (Princeton VSM model-150) is employed to record M Vs H (applied field -20K to 20K) plot of $Ni_{0.5}Co_{0.5}Fe_2O_4$ nanoparticles.

Results and discussion

X-Ray Diffraction analysis

Fig.1(a) shows the x-ray diffraction (XRD) pattern of as-synthesized powder sample obtained from the heat treatment method. A broad diffraction peak is observed, which shows the amorphous nature of as-synthesized powder sample. This may be due to the capping agent (PVP) that encases the metallic cations (Co^{2+}, Ni^{2+}, Fe^{2+}, and Fe^{3+}).

.

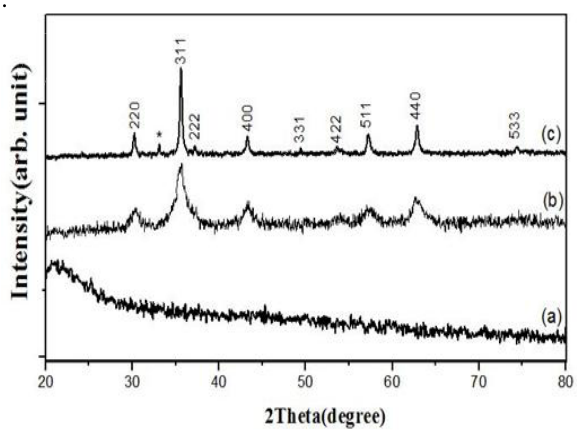

Fig. 1: X-ray diffraction patterns of $Ni_{0.5}Co_{0.5}Fe_2O_4$, **a)** As-synthesized, b) 400ºC, **c)** 600ºC.

Fig.1(b) reveals the x-ray diffraction (XRD) pattern of powder sample that is heat treated at 400ºC for 4 hrs in an electrical furnace. A number of diffraction peaks corresponding to the reflection planes (220), (311), (400), (511) and (440).are observed that are not adequate to confirm the formation of cubic crystal structure. The XRD pattern of the powder sample heat treated at 600ºC for 4 hrs is shown in Fig. 1c) which depicts the clear and sharp peaks corresponding to the reflection planes (220), (222), (311), (400), (422), (511), (440), and (533) (JCPDS card number 01- 088-380), which confirms the formation of face centred cubic spinel structure of cobalt doped nickel ferrite of $Ni_{1-x}Co_xFe_2O_4$ (x=0.5) with α-Fe_2O_3 (hematite phase) as an impure phase indicated by a star **[25, 26]**. The average crystallite size of the cobalt doped nickel ferrite nanoparticles

that were heat treated at 600ºC is calculated as 28 nm using Debye-Scherrer formula **[27]**.

Morphological Analysis

In order to study the particle morphology, microstructure, and imaging of the synthesized nickel cobalt ferrite nanoparticles, the FESEM measurement has been executed. All the powdered samples are palletized for this characterization measurement. The particle morphology and imaging of the as-synthesized, heat treated at 400ºC and 600ºC samples are shown in **Fig. 2(a), Fig. 2(b)**, and **Fig. 2(c)**, respectively.

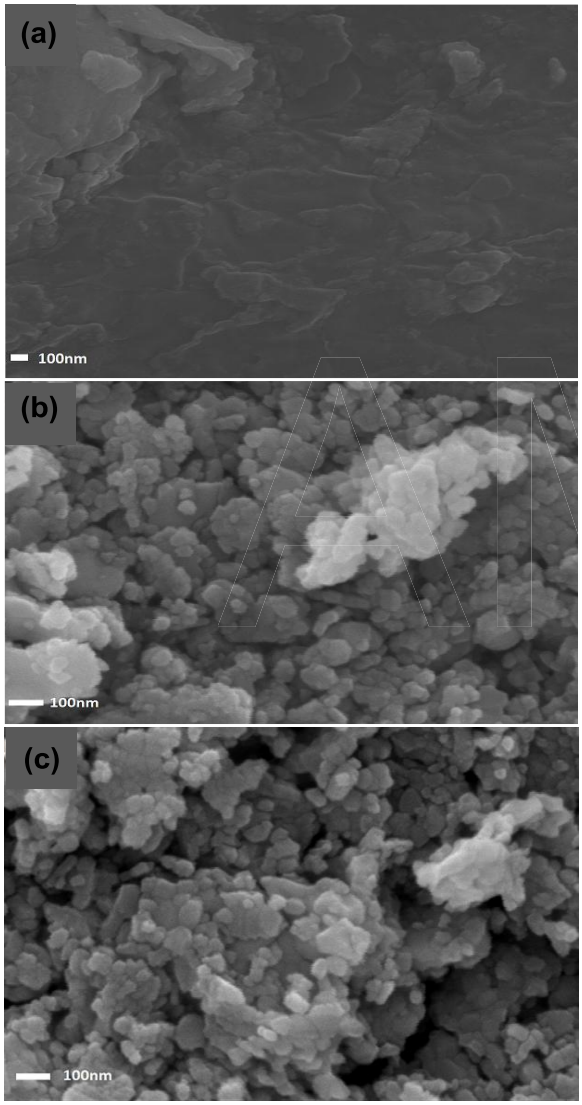

Fig. 2. FESEM images of $Ni_{0.5}Co_{0.5}Fe_2O_4$, a) As-synthesized, b) 400ºC, c) 600ºC.

In the as-synthesized sample (Fig. 2a), the PVP layers that coated the metal cations can be clearly observed. The resulting amorphous nature has already been detected in the XRD results **Fig. 1(a)**. The powdered sample, heat treated at 400ºC for 4hrs (**Fig 2b**) shows $Ni_{0.5}Co_{0.5}Fe_2O_4$ nanoparticles with some PVP impurity. When the as-synthesized sample was heat treated at 600ºC, all the PVP content has been removed **Fig. 2(c)** and the irregular shaped (nearly spherical) nickel cobalt ferrite nanoparticles are obtained with average particle size as 32nm **[28,29]**.

Thermo-Gravimetric Analysis

In order to investigate the temperature up to which the conversion of as-synthesized sample into ferrite nanoparticles occurs, the thermo-gravimetric analysis (TGA) and the differential thermal analysis (DTA) are studied. In. the TGA/DTA curves, three major parts have been observed (**Fig. 3**).

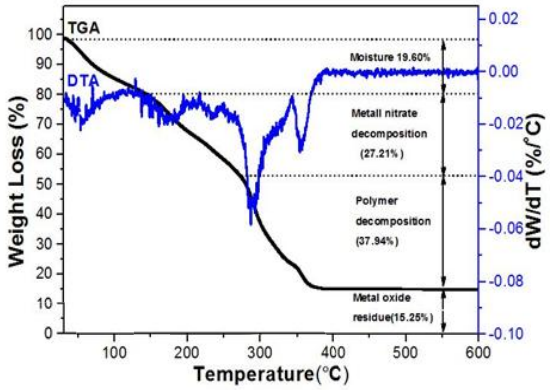

Fig. 3: TGA and DTA curves of as-synthesized $Ni_{0.5}Co_{0.5}Fe_2O_4$ samples.

The first part of the weight loss occurs in the temperature range of 30-150ºC that corresponds to the primary breakdown of the compounds and evaporation of moisture adsorbed in the samples during the preparation of the sample. The second part of the weight loss exists in the temperature range 150-300ºC, which corresponds to the decomposition of metal nitrates. In brief, the spontaneous combustion of nitrates and evaporation of water occurs, where the H_2O, CO, CO_2 NO_x and the nitrate ions provide an oxidizing environment for the combustion of organic compounds. In the third part of the weight loss that ranges from 300-420ºC, a number of mechanisms like the oxidation of organic matters, decomposition of organic salts and degradation of PVP are involved. This degradation mechanism involves both the intra and the intermolecular transfer function **[30-33]**. The rapid weight loss of polymer (degradation) is clearly shown in the DTA curve where the sharp and intense peak is observed in the range of 250-350ºC. Finally, in the last step, at temperature ~ 450ºC and onwards, no weight loss has been found and the cobalt nickel ferrite nanoparticles are formed. The formation of ferrite nanoparticles has been occurred due to the phase transformation phenomenon in the metal oxides. Thus, TGA analysis supports the results obtained in the XRD and SEM analyses.

Magnetization curve Analysis

The ferrites are well known magnetic materials for their excellent magnetic properties. Their magnetic properties depend upon the synthesis route, processing conditions, microstructure, dopants, exchange interaction, chemical composition and anisotropy **[34-37]**. In the as-synthesized sample (**Fig. 4a**), the smaller values of remnant magnetization (M_r), saturation magnetization (M_s) and coercivity (H_c) are obtained because of the PVP which encases the metallic cations as confirmed from the XRD, SEM and TGA results.

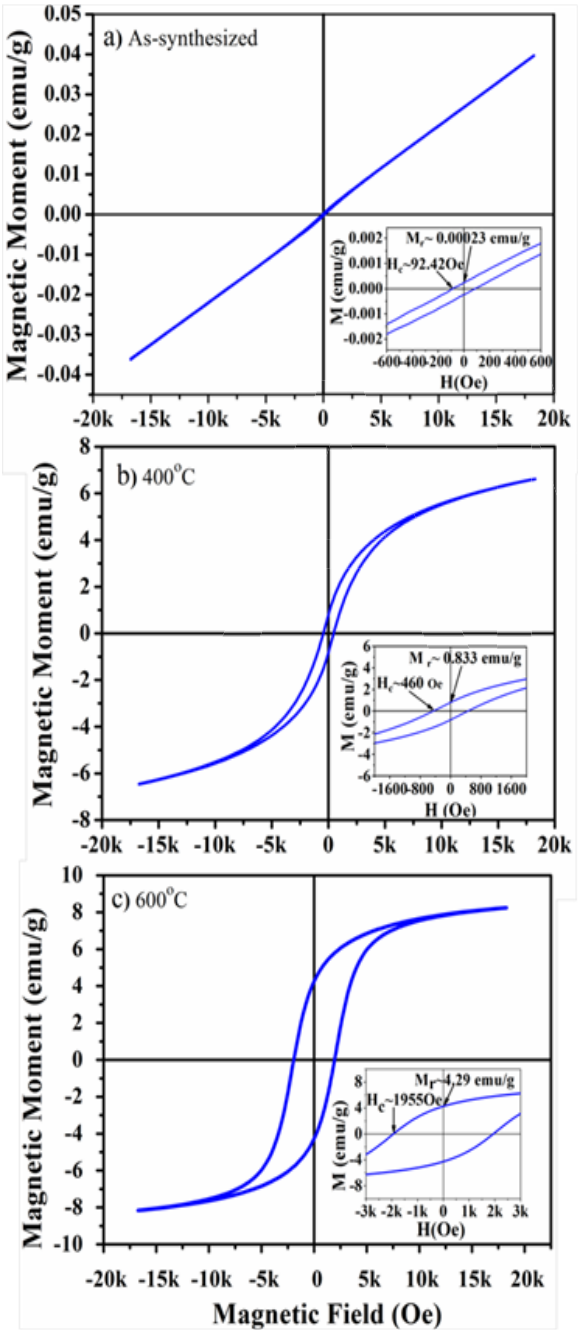

Fig. 4. Magnetization curves of $Ni_{0.5}Co_{0.5}Fe_2O_4$ nanoparticles, (a) As-synthesized, (b) 400ºC, and (c) 600ºC.

In the sample that was heat treated at 400ºC (Fig 4b), an intermediate phase is formed and hence an intermediate value of M_r, M_s and H_c are obtained and the sample that was heat treated at 600ºC (Fig 4c), the higher values of M_r, M_s and H_c are obtained because of the FCC inverse spinel structure of the $Ni_{0.5}Co_{0.5}Fe_2O_4$ nanoparticles. It can be observed (**Table 1**) that the remnant magnetization (M_r), saturation magnetization (M_s) and the coercivity (H_c) are increased with rising the temperature of heat treatment. This enhancement in remnant magnetization and saturation magnetization may be attributed to the distribution of cations at interstices **[38]**. The magneto-crystalline anisotropy that is generally produced from the cobalt doping at the nickel site in $Ni_{1-x}Co_xFe_2O_4$ (x=0.5) may be the potential cause for the increase in the coercivity **[20, 39]**.

Table 1. Magnetic Properties of cubic spinel ferrite.

Sample	H_c(Oe)	M_r(emu/g)	M_s(emu/g)
As-Synthesized	92.42	0.00	0.04
Heat Treated at 400ºC	460	0.83	6.62
Heat Treated at 600ºC	1955	4.29	8.24

Conclusion

The cobalt doped nickel ferrite $Ni_{1-x}Co_xFe_2O_4$ (x=0.5) nanoparticles have been synthesized successfully by the heat treatment method. The face centered cubic inverse spinel structure of $Ni_{1-x}Co_xFe_2O_4$ (x=0.5) nanoparticles sample that were heat treated at 600ºC, has been confirmed from the X-ray diffraction analysis. The particle morphology of the samples has been studied from the field emission scanning electron microscopy, which shows the irregular shape (nearly spherical) and average particle size of the $Ni_{1-x}Co_xFe_2O_4$ (x=0.5) nanoparticles is 32nm (600ºC). In the thermal gravimetric analysis of the as-synthesized sample, it is found that the thermal decomposition occurs up to 400ºC and beyond it, the stable phase of nickel cobalt ferrite nanoparticles is obtained. The TGA result is in accordance with the results obtained in XRD and FESEM analyses. The magnetization curves of the samples reveal that the remnant magnetization (M_r), saturation magnetization (M_s) and the coercivity (H_c) are increased with rising the temperature of heat treatment. The increase in remnant magnetization and saturation magnetization may be attributed to the distribution of metal cations (Ni^{2+}, Co^{2+}, Fe^{3+}) at the interstices, while an increase in coercivity may be due to the magneto-crystalline anisotropy produced in cobalt doped nickel ferrite system.

Acknowledgements

The authors would like to acknowledge Mr. D. D. Pal for XRD and Mr. M. Siva Kumar for the FESEM and VSM measurements.

References

1. Yamamoto, S.; Andou, T.; Kurisu, H.; Matsuura, M.; Doi, T.; Tamari, K.; *J. Magn. Soc. Jpn*., **1998**, *22*, 113.
2. Ortega, A.; Lottini, E.; Fernández, C.; Sangregorio, C.; *Chem. Mater.*, **2015**, *27*, 4048.
3. Kimiabeigi, M.; Widmer, J.; Long, R.; Gao, Y.; Goss, J.; Martin, R.; Lisle, T.; Vizan, J.; Michaelides, A.; Mecrow, B.; *IEEE Trans. Ind. Electron.*, **2016**, *63*, 113.
4. Kim, S.; Park, S.; Park, T.; Cho, J.; Kim, W.; Lim, S.; *IEEE Trans. Ind. Electron.*, **2014**, *61*, 5763.
5. Valenzuela, R.; *Phys. Res. Int.*, **2012**, *2012*, 1.
6. Mathew, D.; Juang, R.; *Chem. Eng. J.*, **2007**, *129*, 51.
7. Renteria, B.; Singhal, R.; Calderon, E.; Perales, O.; Tomar, M.; Banerjee, J.; *Nanotech*., **2007,** *1*, 688.
8. Wu, X.; Yan, S.; Liu, W.; Feng, Z.; Chen, Y.; Harris, V.; *J. Magn. Magn. Mater.*, **2016**, *401*, 1096.
9. Beji, Z.; Sun, M.; Smiri, L.; Herbst, F.; Mangeney, C.; Ammar, S.; *RSC Adv.*, **2015**, *5*, 65010.
10. Singh, C.; Bansal, S.; Kumar, V.; Singhal, S.; *Ceram. Int.*, **2015**, *4*, 3595.
11. Manikandan, A.; Antony, S.; Sridhar, R.; Ramakrishna, S.; Bououdina, M.; *J. Nano. Nanotech.*, **2015**, *15*, 4948.
12. Sanpo N., Wen C., Berndt C, Wang J.; Antibacterial properties of spinel ferrite nanoparticles; Mendez A., (eds); Formatex Research Centre, Spain, **2013**, pp. 239-250.
13. Hudson, R.; *RSC Adv.*, **2016**, *6*, 4262.
14. Sasikala, A.; Unnithan, A.; Park C.; Kim C.; *J. Mater. Chem. B*, **2016**, *4*, 785.
15. Rodrigues, A.; Gomes, I.; Almeida, B.; Araujo, J.; Castanheira, E.; Coutinho, P; *Phys. Chem. Chem. Phys*., **2015**, *17*, 18011.
16. Hoque, S.; Hossain M.; Choudhury, S.; Akhter, S.; Hyder, F.; *Mater. Lett.*, **2016**, *162*, 60.
17. Cullity, B.; Graham, C.; Introduction to Magnetic Materials; Wiley: USA**, 2008**.
18. Goldman, A.; Modern ferrite technology; Springer: USA, **2006**.
19. Smith, J.; Wijn, H.; Ferrites; Wiley: USA, **1959**.
20. Ati, A.; Othaman, Z.; Samavati, A.; *J. Mol. Struct.*, **2013**, *1052*, 177.
21. Reddy, M.; Madhuri, W.; Sadhana, K.; Kim, I.; Hui, K.; Hui, K.; Kumar K.; Reddy, R.; *J. Sol-Gel. Sci. Technol.*, **2014**, *70*, 400.
22. Gaffoor, A.; Ravinder, D.; *Int. J. Eng. Res. Appl.*, **2014**, *4*, 73.
23. Singhal, S.; Singh, J.; Barthwal, S.; Chandra, K.; *J. Solid State Chem.*, **2005**, *178*, 3183.
24. Brito, V.; Cunha, S.; Araujo, F.; Machado, J.; Silva, M.; Nunes, C.; *Ceramica*, **2015**, *61*, 341.
25. Naseri, M.; Saion, E.; Ahangar, H.; Hashim, M.; Shaari, A.; *Powder Technol.*, **2011**, *212*, 80.
26. Naseri, M.; Saion, E.; Ahangar, H.; Shaari, A.; Hashim, M.; *J. Nanomater.*, **2010**, *2010*, 1.
27. Cullity, B.; Elements of X-ray diffraction; Addison Wesley: London, **1978.**
28. Maqsood, A.; Khan, K.; *J. Alloys Compd.*, **2011**, *509*, 3393.
29. Mozaffari, M.; Amighian, J.; Darsheshdar E.; *J. Magn. Magn. Mater.*, **2014**, *350*, 19.
30. Azhari, S.; Diab, M.; *Polym. Degrad. Stab.*, **1998**, *60,* 253.
31. Wang, Z.; Liu, X.; Lv, M.; Chai, P.; Liu, Y.; Meng, J.; *J. Phys. Chem.*, **2008**, *112*, 11292.
32. Sivakumar, P.; Ramesh, R.; Ramanand, A.; Ponnusamy, S.; Muthamizhchelvan, C.; *Mater. Lett.*, **2011**, *65*, 483.
33. Zhang, C.; Shen, X.; Zhou, J.; Jing, M.; and Cao, K.; *J. Sol-Gel Sci. Techn.*, **2007**, *42*, 95.
34. Maqsood, A.; Khan, K.; Rehman, M.; Malik, M.; *J. Alloys Compd.*, **2011**, *509*, 7493.
35. Kadam, R.; Birajdar, A.; Alone, S.; Shirsath, S.; *J. Magn. Magn. Mater*., **2013**, *327*, 167.
36. Bhukal, S.; Bansal, S.; Singhal, S.; *J. Mol. Struct.,* **2014**, *1059*, 150.
37. Bao, L.; Yang, H.; Wang, X.; Zhang, F.; Shi, R.; Liu, B.; Wang, L.; Zhao, H.; *J. Cryst. Growth,* **2011**, *328*, 62.
38. Pulisova, P.; Kovac, J.; Voigt, A.; Raschman, P.; *J. Magn. Magn. Mater*., **2013**, *341*, 93.
39. Yamamoto, H.; Nissato Y.; *IEEE Trans. Magn.*, **2002**, *38*, 3488.

